

# Geostationary Imaging Fabry–Perot Spectrometer (GIFS)

Jeng-Hwa Yee, M. Frank Morgan, R. DeMajistre, William H. Swartz, Elsayed R. Talaat, James F. Garten  
The Johns Hopkins University Applied Physics Laboratory  
11100 Johns Hopkins Road  
Laurel, Maryland 20770 USA

and

Wilbert R. Skinner  
Space Physics Research Laboratory  
University of Michigan  
Ann Arbor, Michigan 48109 USA

**The Geostationary Imaging Fabry–Perot Spectrometer (GIFS) instrument is a next-generation satellite concept to be deployed on a geostationary satellite for continuous hemispheric imaging of cloud properties, including cloud top pressure, optical depth, fraction, and surface reflectance. GIFS uses an innovative tunable imaging triple-etalon Fabry–Perot interferometer to obtain images of high-resolution spectral line shapes of two O<sub>2</sub> B-band lines in solar backscattered solar radiation. The GIFS remote sensing technique takes advantage of the pressure broadening information embedded in the absorption line shapes to better determine cloud properties, especially for those clouds below 5 km. We present a preliminary instrument design, including the general instrument requirements, as well as ongoing work toward an aircraft prototype.**

## I. INTRODUCTION

Earth observations from geostationary orbit are ideal for providing long-term, diurnal, regional coverage of natural phenomena. Long-term measurements of clouds, including their global distribution, cloud top pressure, optical depth, and cloud fraction, are needed to provide inputs to climatological models for global change studies. A compact, low-cost instrument capable of making these measurements is required to meet scientific research objectives for studies of climate in the 21<sup>st</sup> century.

The Geostationary Imaging Fabry-Perot Spectrometer (GIFS) instrument concept is an ideal approach to make cloud property measurements with the desired spatial resolution, accuracy, and revisit time. It uses an innovative tunable imaging triple-etalon Fabry–Perot interferometer (FPI) to obtain hemispheric images of high-resolution spectral line shapes of O<sub>2</sub> Atmospheric band absorption lines in backscattered solar radiation. The GIFS remote sensing technique takes advantage of the pressure broadening information embedded in the absorption line shapes to better determine cloud properties, especially for clouds below 5 km. The GIFS team, based at The Johns Hopkins University Applied Physics Laboratory (JHU/APL) and the University of Michigan (UM), has recently demonstrated the feasibility of this technique using data from the High Resolution Doppler Imager (HRDI) onboard the Upper Atmosphere Research Satellite (UARS) [1]. Lessons learned from this feasibility investiga-

tion have been leveraged to provide the design of GIFS, an optimal cloud-sensing instrument. The versatile GIFS concept can easily be modified to provide many other measurements that are applicable to current scientific objectives.

## II. MEASUREMENT TECHNIQUE

Techniques for the measurement of clouds from space fall into two categories: active and passive remote sensing. Active sensors that transmit microwave or laser light can provide high-resolution vertical information but are limited to point measurements along the satellite track. Passive imagers that measure the natural radiation emitted or scattered by clouds provide much greater horizontal coverage with limited vertical resolution.

The O<sub>2</sub> Atmospheric A, B, and  $\gamma$  ( $X^3\Sigma_g^-b^1\Sigma_g^+$ , 0-0, 1-0, 2-0) band transitions located at around 762, 685, and 637 nm, respectively, have absorption cross sections ideal for probing the atmospheric O<sub>2</sub> density (and thus total density) in the Earth's lower and middle atmosphere. Recent calculations indicate that estimates of cloud top altitudes as well as optical depths can be retrieved from observations of the O<sub>2</sub> Atmospheric bands using a moderate resolution (0.5–6.0-nm) spectrometer. The accuracy of the estimates can be improved by measurements with higher spectral resolution and/or higher signal-to-noise ratio (SNR), where it is possible to characterize the spectral shape of an individual absorption line.

Fig. 1 shows the calculated line shapes for a single O<sub>2</sub> B-band absorption line for a series of clouds of different cloud top pressures. The asymptotic radiance ( $\sim 1.0 \times 10^8$  R/cm<sup>-1</sup>) contains information about the effective optical depth and surface reflectance. The shape, especially the width, of the absorption line contains information about the pressure levels where the scattering/surface reflection occurs. The equivalent width of the absorption line contains the information about the amount of O<sub>2</sub> in the total scattering path. The spectral resolution needed for individual line measurements ( $\sim 0.05$  cm<sup>-1</sup>) is technologically achievable through the use of an FPI.

The GIFS team has investigated the feasibility of retrieving cloud top pressure using nadir-viewing spectral line shape measurements of the O<sub>2</sub> B-band taken by HRDI, a triple-

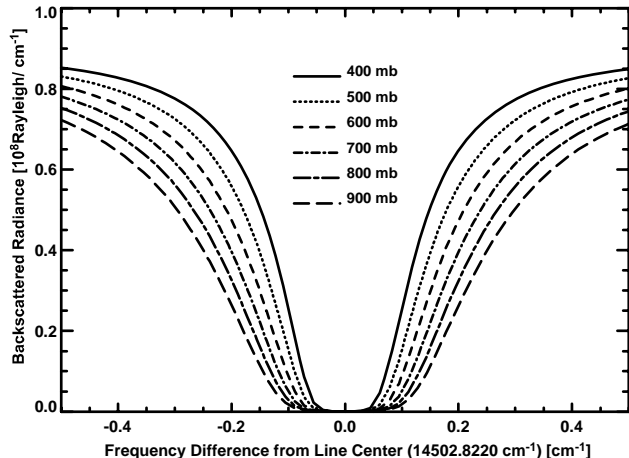


Fig. 1. Cloud backscattered solar radiance for clouds with tops at various pressure levels produced using line parameters from the HITRAN database and using the DISORT radiative transfer algorithm. For each trace, a cloud layer thickness of 100 mb and an optical thickness of 5 were assumed.

etalon FPI onboard the UARS spacecraft. From our HRDI experience, we conclude that there are several advantages of a specially designed FPI measurement technique over its spectrograph counterparts:

- high-resolution absorption line spectra can capture pressure broadening and equivalent width information, yielding more accurate cloud top pressure and optical depth retrievals, especially for low-level cloud conditions;
- high-fidelity calculations of single-line spectra are less computationally expensive, allowing more efficient retrievals;
- individual lines can be selected that are free of contamination from water vapor, solar Fraunhofer lines, effects of temperature variation, and other complications in the data analysis;
- near-global high-spatial/spectral resolution line shape measurements over a 2-D spatial scene can be obtained with a short revisit time by the use of an FPI system operating in an imaging mode.

In order to implement the FPI measurement technique in a daytime imaging mode, we need the following instrument characteristics:

- an optical system that provides an adequate SNR and white light rejection to meet accuracy requirements, while acquiring images fast enough such that cloud features do not change appreciably during the acquisition of spectra;
- adequate spectral resolution to resolve pressure broadening signatures in  $O_2$  line shapes;
- a single  $O_2$  absorption feature suitable for providing cloud property information for various cloud types and heights;
- spatial scan capability to obtain global coverage with physically meaningful spatial resolution.

*A concept for a spaceborne imaging FPI instrument,*

*GIFS, has been developed to provide 2-D cloud properties from high-spectral resolution measurements of the  $O_2$  absorption line in solar backscattered radiation. The baseline  $O_2$  lines selected for the GIFS investigation are the B-band  $P7$  and  $P7$  lines at  $14,502.8219 \text{ cm}^{-1}$  and  $14,504.7954 \text{ cm}^{-1}$  (the closest water vapor line is  $\sim 5 \text{ cm}^{-1}$  away and there is no Fraunhofer feature nearby). These two lines are selected because their absorption cross-sections are relatively insensitive to temperature. Therefore, the pressure levels of the cloud deck are the most important factors determining the absorption line shapes, making these two lines ideal for probing the troposphere, where large temperature variations ( $\sim 100 \text{ K}$ , summer-to-winter, surface-to-tropopause) are expected. Observations from a geostationary platform eliminate the spatial smearing during a spectral scan and the large Doppler shift correction that arises from the relative motion between Earth and the spacecraft, as would be encountered on a low Earth orbit (LEO). Doppler shifts due to wind-driven cloud motion ( $\sim 0.002 \text{ cm}^{-1}$  at the jet stream) are significantly smaller than the width of the absorption line, typically a few tenths of  $\text{cm}^{-1}$ . Furthermore, a geostationary orbit will assure cloud-free observations for surface reflectance measurements for each geophysical footprint within a reasonable time span ( $\sim 1$  week, based on statistics). The following section describes the GIFS design and operational concept.*

### III. GIFS INSTRUMENT DESIGN

Only three FPIs have flown in space: FPI [2], HRDI [3–5] and TIDI [6,7], onboard the DE, UARS, and TIMED spacecraft, respectively. All three are high-resolution FPIs that were primarily designed to measure Doppler shifts of upper atmospheric airglow emission lines. GIFS has substantial innovations on their designs. While the HRDI instrument uses three etalons in tandem with two of the three tunable by the use of piezoelectric posts (DE/FPI and TIDI are single, fixed-plate etalon systems), GIFS is the first spaceborne FPI designed to piezo-scan all three etalons. The TIDI instrument uses a CCD detector but intentionally scrambles the incoming light to remove spatial information (similar to HRDI). GIFS will form spatially coherent images on the CCD detector and will therefore be the first instrument to combine a tunable tripe-etalon FPI (and its high-spectral resolution) with a simultaneous spatial imaging capability. The GIFS instrument consists of a two-axis scanning telescope, a tunable triple-etalon FPI with a CCD detector, and associated electronics. A block diagram of the GIFS instrument is presented in Fig. 2. Fig. 3 shows the optical train of the GIFS instrument. Light from the telescope or from calibration sources is selected by positioning a scene selector mirror. Light is collimated, and passed through a narrow-band filter wheel to select any of several  $O_2$  B-band transitions, spectral calibration lines, or incandescent light. The beam is expanded and passed through a set of three piezoelectrically tuned low-, medium-, and high-resolution etalons (LRE, MRE, HRE). Three etalons in series reduces the sidebands that would occur with one etalon

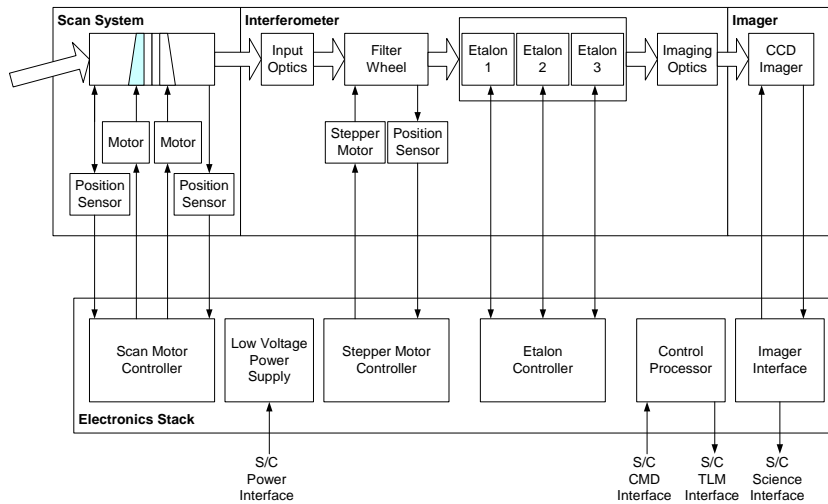


Fig. 2. GIFS instrument block diagram.

when trying to resolve a narrow spectral region within an atmospheric continuum. The beam is finally focused through an imaging telescope onto a CCD detector providing a two-dimensional, spectrally filtered image of the scene. Stepping the etalon gaps in resonance and acquiring a CCD image at each step produces a high-resolution spectrum at each spatial pixel. Coupling the FPI system with a two-axis scan system allows for acquisition of a mosaic of spectral images from a three-axis stabilized spacecraft. An embedded computer controls image collection, tuning/stepping of the etalons, and the pointing system. FPI science and instrument engineering data are sent to the spacecraft via a serial link for storage and downlink. Table I shows the GIFS design specifications and driving requirements determined by trade-off studies between measurement accuracy, spatial resolution, integration time, and spectral coverage.

**Telescope Scan System** Two-axis scanning is accomplished with a baseline wedge scanner approach developed for MOLA (Mars Observer Laser Altimeter), GLAS (Geo-

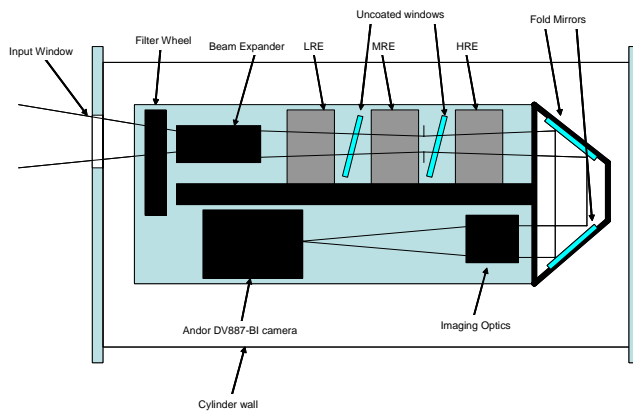


Fig. 3. Optical train of the GIFS instrument. HRE=High Resolution etalon, MRE = Medium Resolution etalon, LRE = Low Resolution etalon.

science Laser Altimeter System) and the lidar system on JIMO (Jupiter Icy Moons). The wedge scanner uses counter-rotating refractive wedges to deflect the line of sight through any desired range of angles about two axes.

**Imaging FPI** The imaging Fabry–Perot optical system consists of a triple-cavity filter ( $\sim 4 \text{ cm}^{-1}$  FWHM), a set of three 150-mm Spectrosil-B etalons, and a CCD detector. The gaps between each etalon are optimized to minimize the amount of white light leaked from the higher-order transmission. All three etalons have a 0.90 reflectivity ZnS–ThF<sub>4</sub> coating at 680 nm, giving rise to a reflectivity finesse of  $\sim 30$ . A system finesse of 20, a conservative estimate to include optical defects, results in an instrument resolution

of  $\sim 0.05 \text{ cm}^{-1}$ . The gaps of these three etalons are piezoelectrically controlled (with Michigan Aerospace Corporation’s (MAC) new patented capacitive feedback scheme described in U.S. Patent #60/268789), and they are individually “tuned” so that all three etalons are in “resonance” and have maximum transmission at the same frequency. The three well-tuned and optically aligned/parallel etalons along with a filter effectively attenuate the background continuum outside the narrow transmission peak, as shown in Fig. 4.

GIFS forms a 2-D image on the detector, with each pixel mapping to a different geographical footprint. Each pixel has a peak transmission at a different resonance wavenumber following a concentric Fabry–Perot fringe pattern. The difference in the resonant wavenumber from the center pixel to another spatial pixel is determined by its incident angle to the etalon plates. For GIFS, the maximum plate incident angle is  $1.345^\circ$  ( $0.95^\circ \times 0.95^\circ$  etalon angular divergence), corresponding to  $3.99 \text{ cm}^{-1}$  difference in resonance frequency between the center pixel and the edge of GIFS field of view (FOV). In other words, operating under this imaging mode, a single GIFS acquisition produces a spectrally filtered image of a 2-D  $3.6^\circ \times 3.6^\circ$  scene, and a high-resolution spectrum at each spatial pixel is accomplished by stepping the etalon gaps in resonance. The details of the spectral scanning technique will be described later.

The Fabry–Perot etalon system is placed in a vacuum housing and thermally controlled to minimize the thermal drift.

**CCD Detector** The GIFS CCD detector is a passively cooled, back-thinned, 1024x1024 frame transfer device, the E2V 4720. The quantum efficiency is  $\sim 0.88$  at 680 nm. The re-imaging optics will focus the instantaneous scene onto this CCD, which will be binned on-chip to produce a 512x512-pixel image. The Fabry–Perot image will be read out at 1 Hz using a 12-bit A/D converter with a read noise of  $\sim 10$  electrons.

TABLE I  
GIFS ENGINEERING PARAMETERS

Engineering Parameters	Driving Requirement	Value
<b>Telescope</b>		
Aperture	throughput	79 mm
Field of view	spatial coverage	3.6°
<b>Filter</b>		
Type	line transmission	3 cavity
Peak transmission	signal to noise	>0.6
Spectral width	off-band rejection	0.4 cm <sup>-1</sup> FWHM
Effective index	spectral shift	2
<b>Interferometer</b>		
# of etalons	off-band rejection	3
Clear aperture	sensitivity	150 mm
Gap thicknesses	spectral resolution, off-band rejection	0.5 cm (H) 0.205 cm (M) 0.0445 cm (L)
Free Spectral Range (FSR)	spectral resolution, off-band rejection	1.0 cm <sup>-1</sup> (H) 2.44 cm <sup>-1</sup> (M) 11.24 cm <sup>-1</sup> (L)
Reflectivities	same as FSR	0.90
System finesse	same as FSR	20
Spectral resolution.	retrieval precision	0.05 cm <sup>-1</sup>
<b>Detector</b>		
Array size	spatial resolution	1024 x 1024
Pixel pitch	angular resolution	13 μm
Read noise	signal to noise	<10 el/read
QE	signal to noise	0.88
Integration time	signal to noise	1 sec
<b>System</b>		
Pixel sensitivity	signal to noise	1.6x10 <sup>-4</sup> el/R/cm <sup>-1</sup> /sec
Pixel resolution	footprint size	0.007°
Acquisition time	signal to noise	1 second
<b>Pointing</b>		
Control	minimize overlap	0.01°
Knowledge	spatial registration	0.001°

**Spectral Scanning Technique** For cloud parameter retrievals, one needs to obtain, at every image pixel, a spectral profile of an O<sub>2</sub> absorption line spanning a spectral range of at least 2 cm<sup>-1</sup> with a spectral sampling interval of <0.05 cm<sup>-1</sup>. Fig. 5 illustrates the technique used to obtain the required spectral scans.

The filter is chosen such that, for a given pixel, the shift in the filter bandpass due to the FOV angle will match the change in the etalon transmission peak frequency. The bottom two panels of Fig. 5 show the filter bandpass for incidence angles corresponding to the center and corner pixels of the CCD, the two limiting cases.

Stepping the interferometer over its tuning range scans the wavenumber seen by different pixels over nearly identical ranges. However, at a given scan position the peak wavenumber varies with radius from CCD center, so there is a 4 cm<sup>-1</sup> shift of the scan from CCD center to corner. For a given pixel, a 2-cm<sup>-1</sup> tuning range centered on the O<sub>2</sub> line

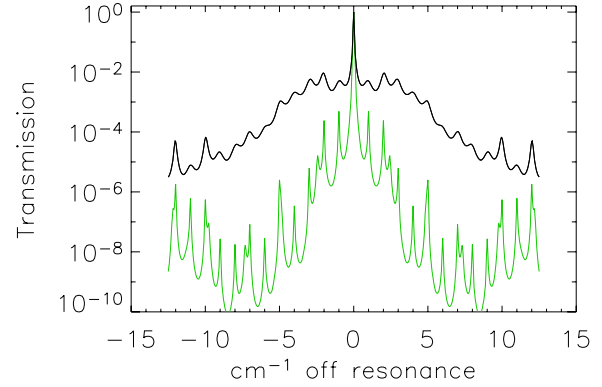


Fig. 4. Calculated GIFS interferometer transmission for ideal etalons (green) and realistic simulation (black), including defects and inter-etalon reflections. Also included in both is the 4-cm<sup>-1</sup> FWHM filter.

visible through the shifted filter bandpass is required. A pair of O<sub>2</sub> lines separated by 1.97 cm<sup>-1</sup> is targeted so that every pixel scans the required interval over at least one of the lines with an etalon scan range of 3.2 cm<sup>-1</sup>. Sampling at a 0.025-cm<sup>-1</sup> interval, each spectral scan requires 128 steps.

Fig. 5 shows the distribution of resonance wavenumbers across the detector at the first, middle, and last steps of the scan. The bottom two panels show the filter transmission spectrum as seen by the center and corner pixels, along with the corresponding interferometer transmission at the three scan steps. The spectral positions of the first and last scan steps are mapped up to the O<sub>2</sub> spectrum in the top panel, showing that the center pixel covers the 14,502.82 cm<sup>-1</sup> line near the end of the scan, while the corner pixel covers the 14,504.80 cm<sup>-1</sup> line near the beginning. The pixel-to-pixel variation of the line coverage phasing drives the necessity to scan a greater overall tuning range than is required for any single pixel.

At each spectral scan step, a single CCD “unit image” is exposed for 1 second. The 128-step spectrum to produce a “spectral image” requires 128 seconds to complete.

**GIFS Operations Concept** GIFS is designed to map cloud properties with 4.4-km resolution over a 120° disk of the Earth (60° in zenith from the geostationary position of the instrument). Coverage can be achieved using a mosaic of these two-dimensional, 512x512-pixel images. Each pixel would project to a 4.4-km square at the Earth, and the Earth disk will be covered by 25 images in a 5x5 mosaic. Given the scanning scheme described above, one entire mosaic takes ~1 hour to acquire.

Concentrating on limited areas for regional studies allows for a much faster mosaic acquisition. For example, North America can be covered by a 2x2 mosaic in ~10 minutes.

GIFS is a next-generation passive imaging instrument that can provide 2-D measurements of cloud top pressure and optical depth. Existing LEO spaceborne passive cloud instrumentation measure horizontal swaths along the satellite

TABLE II  
UNCERTAINTIES FOR A CLOUD WITH A TOP OF 800 MB AND A CLOUD  
BOTTOM AT 900 MB

Cloud optical depth	Optical depth uncertainty	Cloud top pressure uncertainty (mb)	Cloud height uncertainty (m)
1	0.009	24	240
5	0.08	12	126
50	6	8	85

track and must collect data over a day to provide global coverage. GIFS would provide extended monitoring of large sectors of the Earth disk and hemispheric coverage with a spatial resolution of 4.4 km (~4 km for GOES) and a revisit time of roughly an hour (~26 minutes for GOES). Because of its high-resolution O<sub>2</sub> absorption sensing technique, GIFS can provide similar cloud property measurements with greatly improved precision and accuracy and extend the measurement capability for low-lying clouds. GIFS would reduce the uncertainty in comparable cloud top pressure measurements using microwave and infrared radiometry, currently between 0.5 and 1.5 km [8,9] for medium and high clouds. Uncertainties associated with the cloud top pressure from the infrared CO<sub>2</sub> channels of GOES are ~100 mb for low-cloud conditions [10] GIFS would provide significantly improved retrievals, with uncertainties ~20 mb (see Table II).

Similar O<sub>2</sub> absorption techniques for cloud sensing can potentially be achieved by using a spectrograph or Fourier transform spectrometer. However, providing measurements with GIFS spatial resolution, spatial coverage, revisit time, and precision/accuracy is very technologically challenging and prohibitively demanding of spacecraft resources.

#### IV. EXPECTED MEASUREMENT UNCERTAINTY

The GIFS instrument design has been optimized to provide the most precise and accurate cloud property retrievals by challenging all aspects of the instrument technology under cost constraints. This optimization not only has involved a survey of existing cloud measurement techniques and instrument technology but also a series of forward measurement simulations and backward cloud property retrievals. Although the retrieval technique employed here is still rudimentary (i.e., a simple multi-parameter fit), the results provide us a good estimate of the expected accuracy/precision of retrieved cloud properties for any particular instrument design.

Tables II and III summarize the expected GIFS measurement uncertainties for two different cloud decks over open ocean (0.01 surface albedo) at a solar zenith angle and an observer zenith angle of 40°. The error estimates presented above assume knowledge of the surface albedo and the cloud bottom pressure (can be iteratively estimated from cloud type—given cloud top pressure and optical depth). In general, the larger the cloud optical depth, the less sensitive the retrieval is to the uncertainties of these two parameters. A geostationary orbit, in general, will assure cloud-free observa-

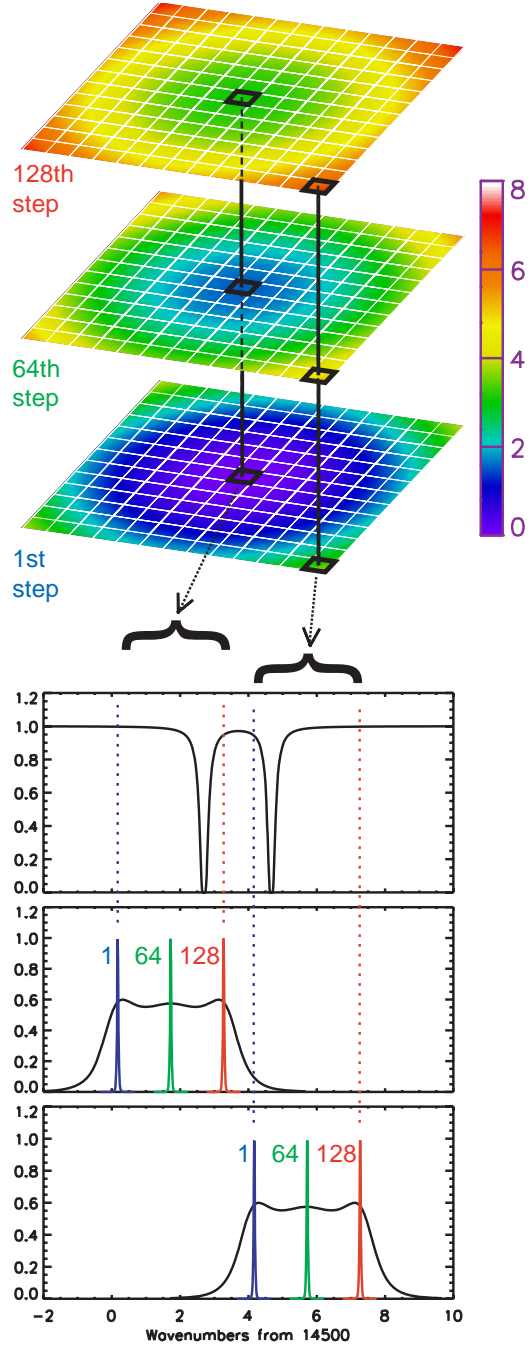


Fig. 5. FPI Scan. The upper three color panels represent the wavenumber resonant across the CCD for the first, middle, and last etalon steps of the 128-step scan. The lower two plots show the etalon resonance (narrow peaks) for the same three steps and their relation to the filter bandpass (black curves) for the center (center plot) and corner (lower plot) pixels. The upper plot shows the O<sub>2</sub> spectrum, with dotted lines indicating the scan ranges of the center and corner pixels. These two pixels correspond to the extreme etalon incidence angles and therefore the extreme limits of the scan ranges.

tions for a good surface albedo measurement for any geographical footprint within a reasonable time span (~1 week). One should be able to use albedo maps generated by GIFS to constrain the retrieval processes without introducing significant systematic error. The systematic errors introduced by

TABLE III  
UNCERTAINTIES FOR A CLOUD WITH A TOP OF 500 MB AND A CLOUD  
BOTTOM AT 600 MB

Cloud optical depth	Optical depth uncertainty	Cloud top pressure uncertainty (mb)	Cloud height uncertainty (m)
1	0.006	15	220
5	0.06	8	116
50	4	5	79

not knowing the cloud bottom pressure can be as large as the reported measurement precisions for optically thin clouds (optical depth of  $\sim 1$ ). For these two types of low clouds, the precisions of GIFS cloud top height measurements are generally  $\sim 100$  m for various cloud optical depths, and slightly larger for thin clouds. It is clear that GIFS can provide critically needed low altitude cloud measurements that are difficult to obtain from current infrared brightness temperature measurements.

It should be noted that the optical depth derived here is only an effective value, i.e., corrected for forward scattering. Our simulations show that there is essentially no information in the backscattered radiance signatures about the scattering phase functions within the clouds. The effective optical depths, however, are most useful for estimating radiative losses in clouds for modeling purposes.

#### V. "GIIP" INSTRUMENT INCUBATOR PROJECT

In order to increase the technical readiness level of the GIFS concept, we have started a NASA Instrument Incubator Program (IIP) project to develop, deploy, and test a GIFS prototype ("GIIP") on a suitable aircraft platform. For this IIP effort, the prototype GIIP/GIFS will provide high-spectral resolution measurements of individual  $O_2$  absorption lines to obtain 2-D maps of cloud top pressure and optical depth. An instrument like GIIP/GIFS has never been developed, flown, and tested. Successful testing and operation of GIIP will provide an opportunity to demonstrate the GIFS instrument concept and measurement capability.

The GIIP effort will develop an FPI system suitable for continuous aircraft flight, long-duration balloons, and perhaps sub-orbital studies. The GIIP instrument will be tested and calibrated in a laboratory environment, and operational experiment control software will be developed to ensure its performance in the aircraft environment. Ground-based observations of clouds will test the instrument as well as  $O_2$  spectroscopy assumptions. Fig. 7 shows the flight configuration of GIIP, in a vibrationally isolated environmental chamber. Flight testing will be done with a three-flight aircraft mini-campaign using a Learjet, which will (1) verify the instrument performance in an aircraft environment, (2) demonstrate the capabilities of GIIP/GIFS for cloud remote sensing applications, and (3) allow us to improve the retrieval technique. In addition to GIIP, we will fly two additional instruments to provide critical correlative measurements: the Langley Airborne A-band Spectrometer (LAABS) for comparison, and the airborne High Spectral Resolution Lidar (HSRL) for validation. HSRL will provide highly accurate measurements of

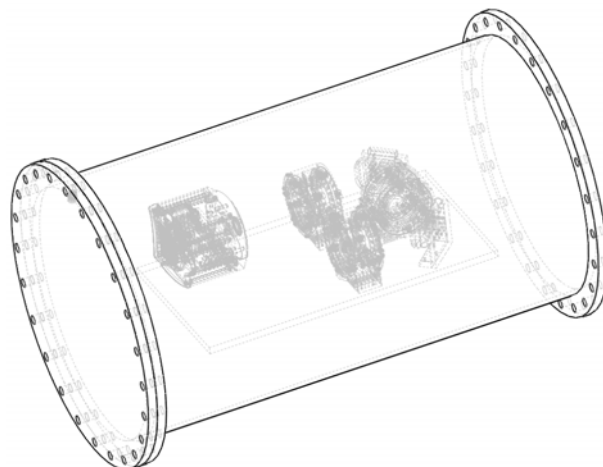


Fig. 7. GIIP instrument within the environmental chamber for aircraft deployment.

cloud height (top and bottom), thickness, and optical depth crucial for validation of the GIIP cloud retrievals. Furthermore, all three flights will occur over ground-based radar or cloud lidar sites. Ideally, we will also attempt under-flights of NASA's A-Train constellation of satellite instruments.

#### VI. CONCLUDING REMARKS

Global observations of low-level clouds are critically needed for long-term climate studies. Differences in the parameterizations of the optical thickness of low clouds used are recognized as the main source of differences in cloud feedback estimates in global circulation models. Currently available measurements from satellite, aircraft, and surface radar indicate that the detection of shallow boundary layer clouds (which produce cooling) remain at the limits of the technique's sensitivity. *This limitation underscores the urgent need to develop alternative technologies to establish a climatology of low clouds. GIFS represents an optical technique that can address this need. A concept for a spaceborne imaging FPI instrument, GIFS, has been developed to provide 2-D cloud properties from high-spectral resolution measurements of  $O_2$  absorption lines in solar backscattered radiation.*

Similar  $O_2$  absorption techniques for cloud sensing can potentially be achieved by using a spectrograph or Fourier transform spectrometer. However, providing measurements with GIFS spatial resolution, spatial coverage, revisit time, and precision/accuracy is very technologically challenging and prohibitively demanding of spacecraft resources.

GIFS has a versatile design that can be adapted easily to obtain additional measurement capabilities. For example, global aerosol optical depth could be obtained with the combination of the  $O_2$  Atmospheric band-derived cloud parameters and infrared channels, from either correlative measurements or through the addition of a co-aligned infrared imager to GIFS, allowing for significantly improved aerosol optical

depth retrievals at high spatial and temporal resolutions high enough to resolve dynamic changes.

In another area of research, a key parameter to understanding the biosphere and its role in the global carbon cycle is a global estimate of the chlorophyll fluorescence (ChlF) emitted naturally from vegetation and phytoplankton. GIFS has the resolution necessary to resolve the Fraunhofer lines and can provide simultaneous estimates of the surface reflectance during clear conditions. The addition of Fraunhofer line-centered filters to the filter wheel would allow GIFS to remotely sense ChlF (William B. Cook, NASA/LARC, private communication).

These are a few of the enhanced measurement capabilities possible with minor modifications of the GIFS instrument.

#### ACKNOWLEDGMENT

We gratefully acknowledge the support of JHU/APL for internal research funding of the initial development of the GIFS instrument concept and continuing support from the NASA Instrument Incubator Program.

#### REFERENCES

- [1] Garten, J. F., W. R. Skinner, A. R. Marshall, and J. M. Raines, An O<sub>2</sub> absorption line method for retrieval of cloud data from the High Resolution Doppler Imager, in preparation, 2004.
- [2] Hays, P. B., T. L. Killeen, and B. C. Kennedy, The Fabry-Perot interferometer on Dynamics Explorer, in *Space Science Instrumentation*, 5, No. 4, pp. 395-416, 1981.
- [3] Hays, P. B., V. J. Abreu, M. E. Dobbs, D. A. Gell, H. J. Grassl, and W. R. Skinner, The High-Resolution Doppler Imager on the Upper Atmosphere Research Satellite, *J. Geophys. Res.*, 98, 10,713-10,723, 1993.
- [4] Grassl, H. J., W. R. Skinner, P. B. Hays, M. D. Burrage, D. A. Gell, A. R. Marshall, D. A. Ortland, and V. J. Abreu, Atmospheric wind measurements with the High Resolution Doppler Imager (HRDI), *J. Spacecraft & Rockets*, 32, No. 1, 169-176, 1995.
- [5] Skinner, W. R., D. A. Gell, A. R. Marshall, P. B. Hays, J. F. Kafkalidis, and D. R. Marsh, The High Resolution Doppler Imager: Instrument performance from late 1991 to mid-1999, *Proc. SPIE*, vol. 3756, 309-315, 1999.
- [6] Killeen T. L., W. R. Skinner, R. M. Johnson, C. J. Edmonson, Q. Wu, R. J. Niciejewski, H. J. Grassl, D. A. Gell, P. E. Hansen, J. D. Harvey, and J. F. Kafkalidis, TIMED Doppler Interferometer (TIDI), *Proceedings of SPIE*, vol. 3756, pp. 289-315, 1999.
- [7] Skinner, W. R., R. J. Niciejewski, T. L. Killeen, S. C. Solomon, D. Gablehouse, Q. Wu, D. Ortland, D. A. Gell, A. R. Marshall, E. Wolfe, Jr., M. Cooper, and J. F. Kafkalidis, Operational performance of the TIMED Doppler Interferometer (TIDI), in *Proc. of SPIE: Optical Spectroscopic Techniques and Instrumentation for Atmospheric and Space Research V*, vol. 5157, pp. 47-57, 2003.
- [8] Frey, R. A., B. A. Baum, W. P. Menzel, S. A. Ackerman, C. C. Moeller, and J. D. Spinhirne, A comparison of cloud top heights computed from airborne lidar and MAS radiance data using CO<sub>2</sub> slicing, *J. Geophys. Res.*, 104, 24,547-24,556, 1999.
- [9] Moroney, C., R. Davies, and J.-P. Muller, Operational retrieval of cloud-top heights using MISR data, *IEEE Transactions on Geoscience and Remote Sensing*, 40, No.7, pp. 1532-40, 2002.
- [10] Li, J., W. P. Menzel, and A. J. Schreiner, Variational retrieval of cloud parameters from GOES sounder long-wave cloudy radiance measurements, *J. of Appl. Meteorol.*, 40, 312-330, 2001.